DOI: 10.61782/fa.2025.0325

FORUM ACUSTICUM EURONOISE 2025

EFFECTS OF ACOUSTIC BLACK HOLE PILLARS ON THE ACOUSTIC ENERGY OF A WATER-FILLED CAVITY

Junjun Li[1] **Jie Deng**[1,2*] **Oriol Guasch** [1*]

[1] Human-Environment Research (HER) group, Department of Engineering, La Salle, Universitat Ramon Llull C/ Quatre Camins 30, 08022 Barcelona, Catalonia, Spain

[2] Chongqing Industry Polytechnic College, 401120 Chongqing, China

ABSTRACT

Acoustic additive black hole (ABH) pillars are known to significantly reduce vibration energy from a host plate. However, little has been done to investigate their performance when the host plate partially encloses a water-filled resonant cavity, a problem that may be important for marine applications. In this work, the ability of ABH pillars to reduce the acoustic energy of the cavity is investigated and compared to that of standard uniform pillars. The elastoacoustic problem is solved using a displacement formulation and Gaussian basis functions are employed to expand all the unknowns of the problem. Boundary and coupling conditions are imposed using the null space method (NSM). The results show that ABH pillars can substantially reduce the acoustic energy of the cavity, outperforming uniform pillars despite their lower mass.

Keywords: *Acoustic black holes, Vibroacoustics, Heavy fluid, Nullspace method*

1. INTRODUCTION

In recent years, acoustic black hole (ABH) technology has garnered a great deal of attention for its effectiveness in mitigating noise in fluid systems. Bowyer and Krylov [1] pioneered experimental investigations into the acoustic radiation of ABH plates, demonstrating that rectangular plates with tapered indentations can effectively reduce acoustic power radiation. Subsequently, the vibroacoustic behavior of ABH plates coupled to air cavities but their connection to heavy fluids has only started recently. In [2], the fluid-structure interaction of ABHs with heavy fluids was addressed by showing the suppression potential of a composite plate-cavity ABH system under heavy fluid excitation, achieving sound pressure level reductions of 4-9 dB above 300 Hz. More recently, the underwater acoustic radiation characteristics of ABH plates were further examined demonstrating superior underwater sound power suppression between the cut-on and critical frequencies [3,4].

Although embedded ABH configurations are the most common, they compromise the original stiffness of the host plate due to thickness adjustment. To overcome these limitations different types of additive ABHs have been proposed. In [5], a dynamic vibration absorber with ABH features (ABH-RBD) was set on a uniform beam achieving effective vibration suppression without compromising structural integrity. Subsequently, symmetric [6] and eccentric [7] circular ABH dynamic vibration absorbers (2D ABH-DVA) were developed to reduce vibrations in uniform plates. Additional research has been conducted on spiral ABHs [8], curved ABHs [9], and ABH pillars [10] as additive structures.

In this study, we propose to place multiple ABH pillars on a uniform beam coupled to a cavity to reduce noise in a cavity filled with heavy fluid. The equations of motion for the fluid-structure coupling system are established from the displacement formulation in [11], using Gaussian basis functions (GEM expansion method in [12–14]) and the nullspace method (NSM) [15] to impose boundary coupling conditions. Finally, the noise reduction capability of the proposed configuration is computed.

**Corresponding author*: *oriol.guasch@salle.url.edu, jie.deng@salle.url.edu.*

2. THEORETICAL MODEL

2.1 Problem description

As illustrated in Fig. 1, to mitigate the noise inside a water-filled cavity with dimensions $L \times L_c$ (highlighted in the blue region), multiple ABH pillars are uniformly mounted on a uniform beam with thickness h_p. The thickness profile of each ABH pillar follows a power-law distribution given by $h_a(x) = \varepsilon x^m + h_c$, where $\varepsilon = (h_a - h_r)/r_{\text{abh}}^m$. At the ends of the ABHs, some damping layers $r_d \times h_d$ (highlighted in the brown region) have been attached to favor energy dissipation. The geometry and material parameters of the coupled system are detailed in Tab. 1.

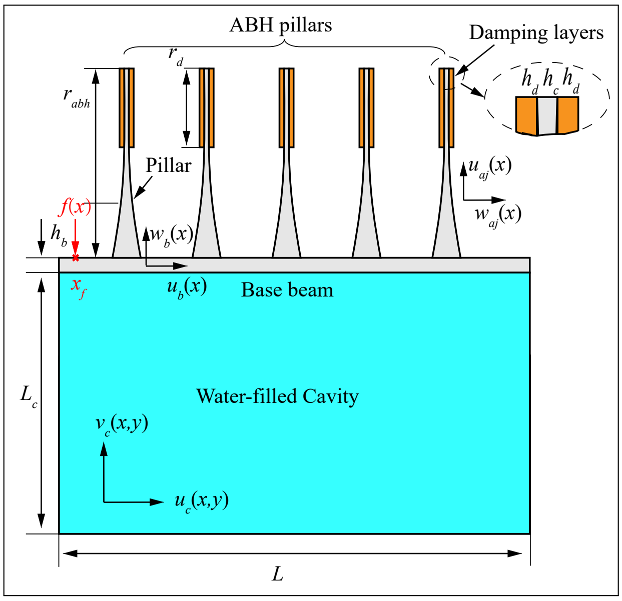

Figure 1. Illustration of the base beam with ABH pillars coupled to a cavity. The blue region indicates the cavity filled with water, while the brown regions represent the damping layers.

2.2 Fluid-Structure Interaction Model

The displacements are represented by variables $u_c(x, y)$, $v_c(x, y)$ for the fluid within the cavity and by $w_b(x, t)$, $u_b(x, t)$ for the uniform beam, respectively. Similarly, the flexural and longitudinal displacements of the ABH pillars can be expressed as $w_{aj}(x, t)$ and $u_{aj}(x, t)$, where $j = 1, 2, \ldots, 5$ denotes the index of the ABH pillars. They are

Table 1. Geometry and material parameters of the coupled system.

Geometry parameters	Material parameters
$L_{cx} = L_b = 0.8\,\text{m}$	$\rho_c = 1000\,\text{kg/m}^3$
$L_{cy} = 0.6\,\text{m}$	$c_c = 1500\,\text{m/s}$
$h_b = h_a = 5\,\text{mm}$	$\eta_c = 0.02$
$m = 2$	$\rho_b = \rho_a = 7800\,\text{kg/m}^3$
$r_{\text{abh}} = 0.4\,\text{m}$	$E_b = E_a = 210\,\text{GPa}$
$\varepsilon = 0.028\,\text{m}^{-1}$	$\eta_b = \eta_a = 0.005$
$h_r = 0.5\,\text{mm}$	$\rho_d = 950\,\text{kg/m}^3$
$r_d = 0.2\,\text{m}$	$E_d = 5\,\text{GPa}$
$h_d = 1\,\text{m}$	$\eta_d = 0.5$

expanded as

$$u_c = \boldsymbol{C}^\top(t)\partial_x\boldsymbol{\varphi}_c(x,y), v_c = \boldsymbol{C}^\top(t)\partial_y\boldsymbol{\varphi}_c(x,y), \quad (1)$$

$$w_b = \boldsymbol{B}_1^\top(t)\boldsymbol{\varphi}_{b1}(x), u_b = \boldsymbol{B}_2^\top(t)\boldsymbol{\varphi}_{b2}(x), \quad (2)$$

$$w_{aj} = \boldsymbol{A}_{j1}^\top(t)\boldsymbol{\varphi}_{aj1}(x), u_{aj} = \boldsymbol{A}_{j2}^\top(t)\boldsymbol{\varphi}_{aj2}(x), \quad (3)$$

where $\boldsymbol{\varphi}_c(x, y) = \boldsymbol{\alpha}(x) \otimes \boldsymbol{\beta}(y)$ are 2D Gaussian functions for the 2D cavity, $\boldsymbol{\varphi}_{b1}(x)$, $\boldsymbol{\varphi}_{b2}(x)$, and $\boldsymbol{\varphi}_{aj1}(x)$, $\boldsymbol{\varphi}_{aj2}(x)$ $(j = 1, 2, \ldots, 5)$ are the 1D Gaussian functions for the base beam and the five ABH pillars, respectively. $\boldsymbol{C}$, $\boldsymbol{B}_1$, $\boldsymbol{B}_2$, $\boldsymbol{A}_{j1}$, and $\boldsymbol{A}_{j2}$ are the coefficient vectors to be determined. The assembled coefficients are defined as $\boldsymbol{q} := [\boldsymbol{C}, \boldsymbol{B}_1, \boldsymbol{B}_2, \boldsymbol{A}_j]$, where $\boldsymbol{A}_j := [\boldsymbol{A}_{j1}, \boldsymbol{A}_{j2}]$.

The Lagrangian of the coupled system is the summation of the Lagrangians of its three components, namely, the cavity, the uniform beam, and the five ABH pillars. This leads to,

$$\mathcal{L} = T_c + T_b + T_a - U_c - U_b - U_a, \quad (4)$$

where T_i and U_i $(i = a, b, c)$ represent the kinetic energy and potential energy of each structure.

By substituting the above expressions into the Euler-Lagrange equations, we can derive the equations of motion,

$$(\boldsymbol{K} - \omega^2\boldsymbol{M})\boldsymbol{Q} = \boldsymbol{0}, \quad (5)$$

where $\boldsymbol{K}$ and $\boldsymbol{M}$ are the stiffness and mass matrices, respectively. However, the above derivation does not explicitly consider the essential boundary conditions of the cavity and the uniform beam, nor the coupling ones at the substructure interfaces. These are accounted for by means of the nullspace method.

The three walls of the cavity are rigid, which implies,

$$u_c(0,y)=0,\quad u_c(L_x,y)=0,\quad v_c(x,0)=0. \tag{6}$$

As for the base beam, it is simply supported on the cavity and coupled with its the upper boundary. The ABH pillars and the uniform beam are coupled at intervals of $d = L_b/6$. These conditions are described by the following equations:

$$w_b(0)=0,\quad w_b(L_x)=0, \tag{7}$$
$$u_b(0)=0,\quad u_b(L_x)=0, \tag{8}$$
$$w_b(x)=v_c(x,L_y), \tag{9}$$
$$w_b(x_j)=u_{aj}(0),\quad u_b(x_j)=w_{aj}(0), \tag{10}$$
$$\partial_x w_b(x_j)=-\partial_x w_{aj}(0), \tag{11}$$

where x_j denotes the connection points of the j-th ABH pillar on the base beam ($j=1,2,\dots,5$).

Substituting Eqn. (1) to Eqn. (3) into Eqn. (6) to Eqn. (11), we obtain,

$$\boldsymbol{\Xi Q} =: \boldsymbol{\Phi}^\top \boldsymbol{Q} = \boldsymbol{0}, \tag{12}$$

where $\boldsymbol{\Xi}$ is the matrix form of the above constraints.

To avoid numerical instabilities, we square and integrate Eqn. (12) over the interface domain, which yields,

$$\boldsymbol{Q}^\top \left[\int \boldsymbol{\Phi}^\top \boldsymbol{\Phi}\, \mathrm{d}x,\right] \boldsymbol{Q} =: \boldsymbol{Q}^\top \boldsymbol{\Psi} \boldsymbol{Q} \tag{13}$$

where, we have defined matrix $\boldsymbol{\Psi}$ is the constant constraint matrix. Finding a basis for the nullspace $\mathcal{N}(\boldsymbol{\Psi})$, we can express $\boldsymbol{Q}$ as $\boldsymbol{Q} = \boldsymbol{Zk}$, with $\boldsymbol{Z}$ containing the nullspace eigenvectors and $\boldsymbol{k}$ being the coefficient vector. Substituting into the equation of motion, Eq. (5), we arrive at,

$$\left(\overline{\boldsymbol{K}} - \omega^2 \overline{\boldsymbol{M}}\right) \boldsymbol{k} = \boldsymbol{0}, \tag{14}$$

where $\overline{\boldsymbol{K}} = \boldsymbol{Z}^\top \boldsymbol{KZ}$ and $\overline{\boldsymbol{M}} = \boldsymbol{Z}^\top \boldsymbol{MZ}$, represent the coupled stiffness and mass matrices, respectively.

3. NUMERICAL RESULTS

To evaluate the performance of ABH pillars in reducing noise inside the cavity, a unit point force is applied at the left x_f of the uniform beam, see Fig. 1.

In Fig. 2, we first present the mean square velocity (MSV) of the host beam. It is observed that if ABH pillars are attached to it instead of uniform (UNI) pillars, the vibration becomes significantly reduced. On the other hand, Fig. 3 presents the acoustic energy ($E = T_c + U_c$) within the cavity. The results indicate again that ABH pillars are more effective than uniform pillars over almost the entire frequency range.

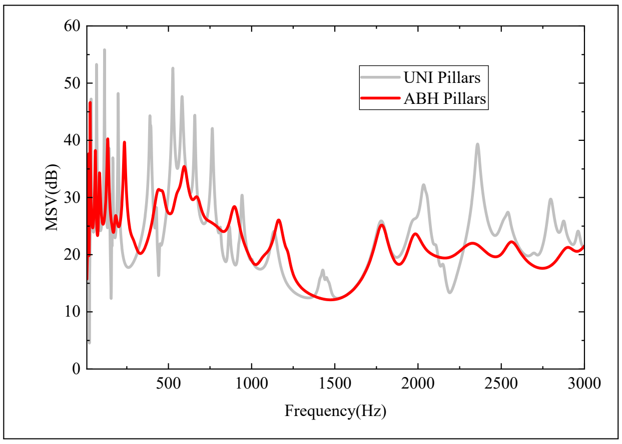

Figure 2. Mean square velocity (MSV) of the host beam.

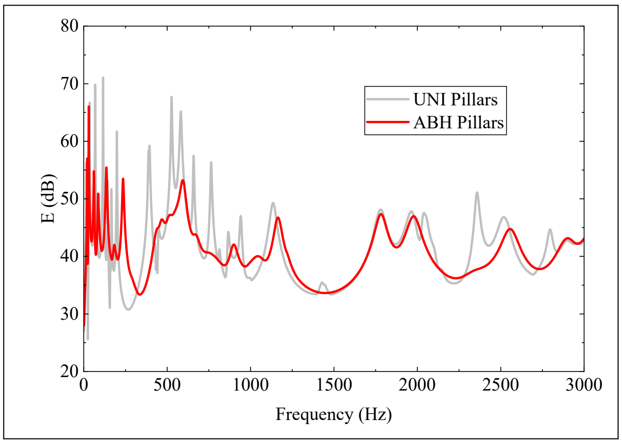

Figure 3. Acoustic energy in the water-filled cavity.

4. CONCLUSION

This paper proposes attaching ABH pillars to host plate to reduce noise transmission inside a heavy-fuid filled cavity. The displacements of the ABH pillars, the base beam, and the fluid have been represented using the Gaussian expansion method (GEM), while the nullspace method (NSM) has been employed to impose the essential boundary and continuity conditions of the problem. The results indicate that ABH pillars can significantly dampen the vibrations of the uniform beam and reduce the energy transmission to the cavity, thus showing excellent noise reduction capability.

5. ACKNOWLEDGMENTS

The authors thank the fund by the China Scholarship Council (CSC No. 202406050053). J. Deng acknowledges the support received by the National Natural Science Foundation of China (52301386), and the support of the Beatriu de Pinós postdoctoral program of the Department of Research and Universities of the Generalitat of Catalonia (2022 BP 00027). O. Guasch acknowledges the support of the Generalitat de Catalunya (Departament de Recerca i Universitats) through grant 2021 SGR 1396 awarded to the HER group.

6. REFERENCES

[1] E. Bowyer and V. V. Krylov, "Experimental study of sound radiation by plates containing circular indentations of power-law profile," *Applied Acoustics*, vol. 88, pp. 30–37, 2015.

[2] D. Wu, M. Yu, Q. Shen, D. Li, and Z. Bai, "Investigation on the characteristics of flow-induced vibration and noise of acoustic window with embedded compound acoustic black holes," *Applied Acoustics*, vol. 228, p. 110376, 2025.

[3] J. Deng, N. Gao, X. Chen, H. Pu, and J. Guo, "Underwater sound radiation from a mindlin plate with an acoustic black hole," *Ocean Engineering*, vol. 278, p. 114376, 2023.

[4] L. Ma and L. Cheng, "Vibration and sound radiation of an acoustic black hole plate immersed in heavy fluid," *The Journal of the Acoustical Society of America*, vol. 154, no. 1, pp. 179–190, 2023.

[5] T. Zhou and L. Cheng, "A resonant beam damper tailored with acoustic black hole features for broadband vibration reduction," *Journal of Sound and Vibration*, vol. 430, pp. 174–184, 2018.

[6] H. Ji, N. Wang, C. Zhang, X. Wang, L. Cheng, and J. Qiu, "A vibration absorber based on two-dimensional acoustic black holes," *Journal of Sound and Vibration*, vol. 500, p. 116024, 2021.

[7] H. Ji, X. Zhao, N. Wang, W. Huang, J. Qiu, and L. Cheng, "A circular eccentric vibration absorber with circumferentially graded acoustic black hole features," *Journal of Vibration and Acoustics*, vol. 144, no. 2, p. 021014, 2022.

[8] S. Park, J. Y. Lee, and W. Jeon, "Vibration damping of plates using waveguide absorbers based on spiral acoustic black holes," *Journal of Sound and Vibration*, vol. 521, p. 116685, 2022.

[9] J. Deng and N. Gao, "Broadband vibroacoustic reduction for a circular beam coupled with a curved acoustic black hole via nullspace method," *International Journal of Mechanical Sciences*, vol. 233, p. 107641, 2022.

[10] J. Deng, N. Gao, and X. Chen, "Ultrawide attenuation bands in gradient metabeams with acoustic black hole pillars," *Thin-Walled Structures*, vol. 184, p. 110459, 2023.

[11] J. Deng, O. Guasch, and L. Maxit, "A displacement formulation for coupled elastoacoustic problems that preserves flow irrotationality," *Journal of Sound and Vibration*, vol. 597, p. 118815, 2025.

[12] J. Deng, L. Zheng, P. Zeng, Y. Zuo, and O. Guasch, "Passive constrained viscoelastic layers to improve the efficiency of truncated acoustic black holes in beams," *Mechanical Systems and Signal Processing*, vol. 118, pp. 461–476, 2019.

[13] J. Deng, L. Zheng, O. Guasch, H. Wu, P. Zeng, and Y. Zuo, "Gaussian expansion for the vibration analysis of plates with multiple acoustic black holes indentations," *Mechanical Systems and Signal Processing*, vol. 131, pp. 317–334, 2019.

[14] J. Deng, O. Guasch, and L. Zheng, "Ring-shaped acoustic black holes for broadband vibration isolation in plates," *Journal of Sound and Vibration*, vol. 458, pp. 109–122, 2019.

[15] J. Deng, Y. Xu, O. Guasch, N. Gao, and L. Tang, "Nullspace technique for imposing constraints in the Rayleigh–Ritz method," *Journal of Sound and Vibration*, vol. 527, p. 116812, 2022.